Buried selectively-oxidized AlGaAs structures grown on nonplanar substrates

P. C. Ku, J. A. Hernandez and C. J. Chang-Hasnain

Department of Electrical Engineering and Computer Science, University of California at Berkeley
175M Cory Hall, Berkeley, CA 94720, U.S.A.

peicheng@eecs.berkeley.edu

We demonstrate a novel buried oxide grating structure formed by selectively-oxidized $Al_xGa_{1-x}As$ grown on nonplanar substrates using low-pressure MOCVD for the first time. Localized aluminum content variation in AlGaAs is obtained with MOCVD growth on nonplanar substrate. Buried aluminum oxide/semiconductor distributed feedback structure is achieved with selective oxidation of these AlGaAs layers. We fabricated a resonant-cavity-enhanced photodetector with the imbedded buried-oxide structure and measured the photodetector responsivity spectrum.

OCIS codes: (160.6000) Semiconductors; (050.1950) Diffraction Gratings

References and links

1. K. D. Choquette et al., "Advances in selective wet oxidation of AlGaAs alloys," IEEE. J. Sel. Top. Quantum Electron. **3**, 916-926 (1997).
2. M. S. Wu, G. S. Li, W. Yuen and C. J. Chang-Hasnain, " Widely Tunable 1.5μm micromechanical optical filter using AlOx/AlGaAs DBR," Electron. Lett. **33**, 1702-1703 (1997).
3. L. D. Westbrook, I. D. Henning, A. W. Nelson, and P. J. Fiddyment, "Spectral properties of strongly coupled 1.5mm DFB laser diodes," IEEE J. Quantum Electron. **21**, 512-518 (1985).
4. S. Oku, T. Ishii, R. Iga, and T. Hirono, "Fabrication and performance of AlGaAs-GaAs distributed Bragg reflector lasers and distributed feedback lasers utilizing first-order diffraction gratings formed by a periodic groove structure," IEEE J. Sel. Top. Quantum Electron. **5**, 682-687 (1999).
5. W. Pan, H. Yaguchi, K. Onabe, R. Ito, and Y. Shiraki, "Composition profile of an AlGaAs epilayer on a V-grooved substrate grown by low-pressure metalorganic vapor phase epitaxy," Appl. Phys. Lett. **67**, 959-961 (1995).
6. L. Hofmann, D. Rudloff, I. Rechenberg, A. Knauer, J. Christen, and M. Weyers, "(AlGa)As composition profile analysis of trenches overgrown with MOVPE," J. Crystal Growth **222**, 465-470 (2001).
7. E. Kapon, "Lateral pattering of quantum well heterostructures by growth on nonplanar substrates," in *Semiconductors and Semimetals vol. 40 Epitaxial Microstructures*, A. C. Gossard, ed. (Academic Press, San Diego, Ca. 1994).
8. R. L. Naone, E. R. Hegblom, B. J. Thibeault, and L. A. Coldren, "Oxidation of AlGaAs layers for tapered apertures in vertical-cavity lasers," Electron. Lett. **33**, 300-301 (1997).
9. S. Noda, N. Yamamoto, M. Imada, H. Kobayashi, and M. Okano, "Alignment and stacking of semiconductor photonic bandgaps by wafer-fusion," J. Lightwave Technol. **17**, 1948-1955 (1999).

1. Introduction

High aluminum (Al) content $Al_xGa_{1-x}As$ is known to be controllably oxidizable under elevated temperature in the presence of water vapor [1]. Oxidized $Al_xGa_{1-x}As$ exhibits properties that make it desirable for device applications [1, 2], such as the oxidation rate being highly selective on aluminum composition, electrically insulating and a low refractive index. Such characteristics make the aluminum oxide (AlOx) a desirable material choice for making efficient grating structures.

State-of-the-art distributed feedback (DFB) lasers and distributed Bragg reflector (DBR) lasers typically have low efficiency gratings, due to small refractive index differences

#1503 - $15.00 US Received July 29, 2002; Revised September 12, 2002

obtained with lattice-matched III-V compound materials. As a result, a long grating structure is required to generate a sufficient reflectivity. Furthermore, the resulting stopband is much narrower than the gain bandwidth, leading to dual mode lasing or a low side mode suppression ratio (SMSR). A grating made with materials with a large index difference, on the other hand, can provide single longitudinal mode operation and a narrower linewidth [3] but often requires a deeply etched semiconductor / air surface structure [4]. Such structures tend to exhibit high defects, and difficulties in process control and device integration.

In this paper, we propose and demonstrate a novel buried oxide grating structure formed by selectively-oxidized $Al_xGa_{1-x}As$ layers grown on nonplanar substrates. The basic idea leverages the fact that the selective oxidation rate depends strongly on Al composition and that Al composition varies for AlGaAs grown on a nonplanar substrate. We fabricated a buried AlOx grating for the first time. The potential advantages of this grating structure include high coupling efficiency, large stop-band, controllable process and facilitation for monolithic integration. In addition, gain and loss coupled gratings can be made by electrically pumping through the unoxidized parts of the grating structure. Potential applications include microcavity DFB lasers, tunable lasers, and various microstructure waveguide devices.

2. Epitaxial Growth

Low Al content $Al_xGa_{1-x}As$ grown on nonplanar substrates is known to have lateral chemical composition variation on different exposed crystal facets [5, 6]. However, high Al content $Al_xGa_{1-x}As$ ($0.9 < x < 1$) ternary compounds grown on nonplanar substrates have not, to the best of our knowledge, been investigated before. Here, we report the properties of buried $Al_xGa_{1-x}As$ ($0.9 < x < 1$) structures on nonplanar substrates.

The substrate was first patterned by optical lithography and the trenches were formed by H_2SO_4:H_2O_2:H_2O (1:8:160) etchant. The trench depths varied from 125nm to 500nm with periods of 4μm to 10μm and a 50% duty-cycle. Immediately before overgrowth, the sample was cleaned by the concentrated HCl solution for 2 minutes and rinsed by DI water. The overgrowth was performed in our Emcore D-75 low-pressure metal-organic chemical vapor deposition (MOCVD) chamber. Tertiarybutylarsine (TBA), triethylgallium (TEGa) and trimethylalluminum (TMAl) were precursors for $Al_xGa_{1-x}As$. The growth pressure and growth rate for $Al_xGa_{1-x}As$ layers were 90mbar and 4.8μm/hour, respectively. V/III ratio was controlled at 12 or 24 for most of the samples. The growth temperature was varied between 580°C and 640°C. The Al solid composition at the planar region was determined by high-resolution x-ray diffractometry (HRXRD). The layer thickness and material quality were examined by a scanning electron microscope (SEM) equipped with a backscattered electron detector. The Al composition x in $Al_xGa_{1-x}As$ ranged from 0.9 to 1. All the growths were performed on (100) GaAs substrates.

To examine the thickness enhancement on different crystal facets, we grew four pairs of GaAs / $Al_xGa_{1-x}As$ thin layers, each with nominal thickness of 80nm and Al composition $x = 0.92$ at the planar region. The cross-sectional SEM images in Fig.1 showed that the $Al_xGa_{1-x}As$ layer thickness was enhanced on higher Miller-index planes both for [01-1]- and [011]-aligned trenches. Fig.1(a) and (b) are two samples both with [01-1]-aligned trenches but were grown at two different temperatures. More layer thickness enhancement can be observed when the growth temperature was lowered from 640°C to 600°C. A typical enhancement ratio of two was obtained. Due to the thickness enhancement on the two sidewalls of the trench, the convergence of higher Miller-index planes can be seen in Fig.1(c). The thickness enhancement is mainly due to higher Al composition at the sidewall. Since $Al_xGa_{1-x}As$ ($x > 0.4$) is an indirect-bandgap material, neither photoluminescence nor cathodoluminescence can be applied to determine the actual Al composition profile. In the next section, we will use the property of high selectivity of $Al_xGa_{1-x}As$ oxidation rate on Al composition to observe indirectly an enhanced Al composition on the sidewall.

#1503 - $15.00 US Received July 29, 2002; Revised September 12, 2002

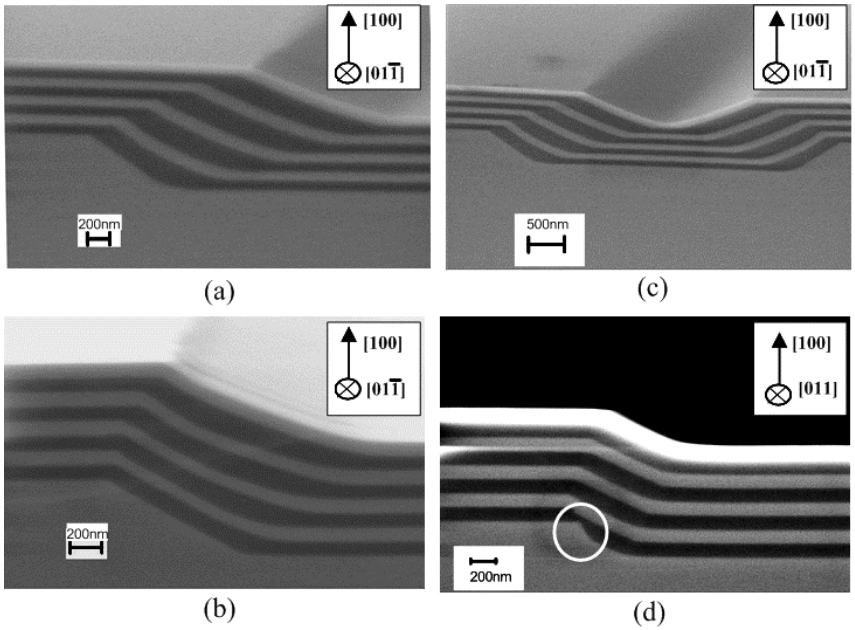

Fig. 1. SEM cross-sectional views of four different sample each with four pairs of GaAs/AlGaAs. Darker regions are AlGaAs layers. Samples (a) and (b) have trenches along [01-1] directions but were grown at two different temperatures, 600°C for (a) and 640°C for (b). The thickness enhancement ratios between the sidewall and the planar region for samples (a), (b) and (d) are 2.20, 1.32 and 1.17, respectively. Sample (c) shows the convergence of two sidewalls. Sample (d) has the trench aligned along [011] direction. The no-growth plane (111)B is circled in (d) too. The nominal aluminum for all these samples is 0.92.

As shown in Fig.1(d), thickness enhancement existed although it was not appreciable (enhancement ratio ~1.17) for [011]-direction trenches as well. (111)B no-growth planes were observed and marked with a circle in Fig.1(d). This is due to a group-V rich growth condition [7].

3. Oxidation

After overgrowth, a ridge waveguide structure was defined to expose the $Al_xGa_{1-x}As$ layer and the sample was thermally oxidized at a steam temperature of 450°C or 470°C. The carrier gas for the oxidation process was N_2 with a flow rate of 500sccm. The oxidation rate was controlled at 0.5μm/min for nominal Al composition x = 0.92 and 0.95μm/min for x = 0.97. The oxide front pattern was observed both by the optical microscope (bright field) and the SEM with the backscattered electron detector. The top views are shown in Fig.2. The oxide front is uniform at the region without gratings and forms a sharp-angled saw-tooth pattern at the nonplanar region due to high selectivity of the oxidation rate on Al composition. An average of 25% to 35% higher oxidation rate was obtained for $Al_xGa_{1-x}As$ at the intersections between the sidewalls and the crests of the gratings. It is also interesting to note that the oxidation rate for $Al_xGa_{1-x}As$ in the region without gratings is much slower, forming a natural tapered waveguide structure. We think this is due to an enhanced lateral oxidation [8], along the direction perpendicular to the oxidant flow, in the region with gratings.

#1503 - $15.00 US Received July 29, 2002; Revised September 12, 2002

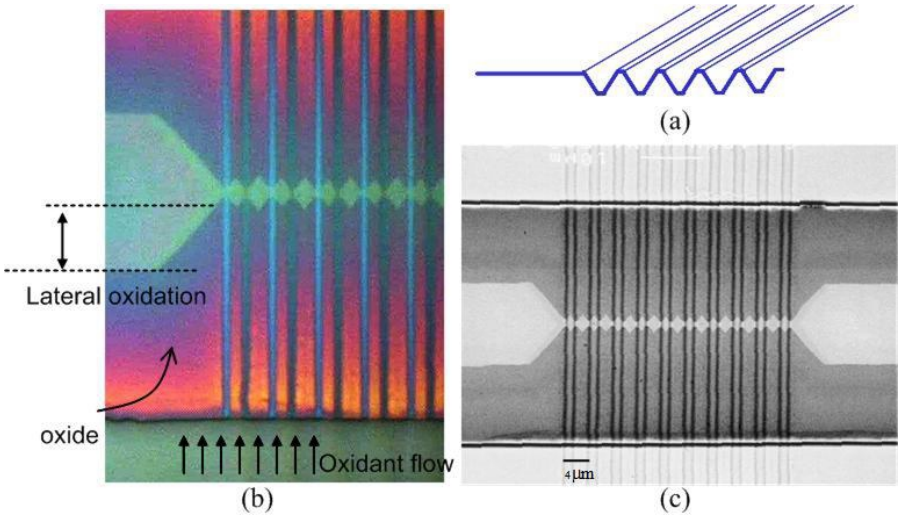

Fig. 2. Oxide front pattern of $Al_xGa_{1-x}As$ on nonplanar substrates with trenches aligned in the [01-1] direction. (a) A schematic shows the nonplanar substrate . (b) Oxide front pattern bright field image. (c) Oxide front pattern top view from the SEM with the backscattered detector.

Similar laterally varying oxidation rates were attained for both [01-1]- and [011]- aligned trenches as shown in Fig.3(a), which suggests this processing technique can be applied to the creation of cross-wire type photonic bandgap structures [9].

The period of the grating after oxidation is only half of that defined by the lithography before the overgrowth as shown in Fig.3(b). This is because in each grating period, there are two symmetric higher Miller-index planes that result in higher oxidation rates. The doubling of the spatial frequency of the grating makes it applicable to fabricate high-resolution distributed-feedback devices with lower-resolution lithography technique.

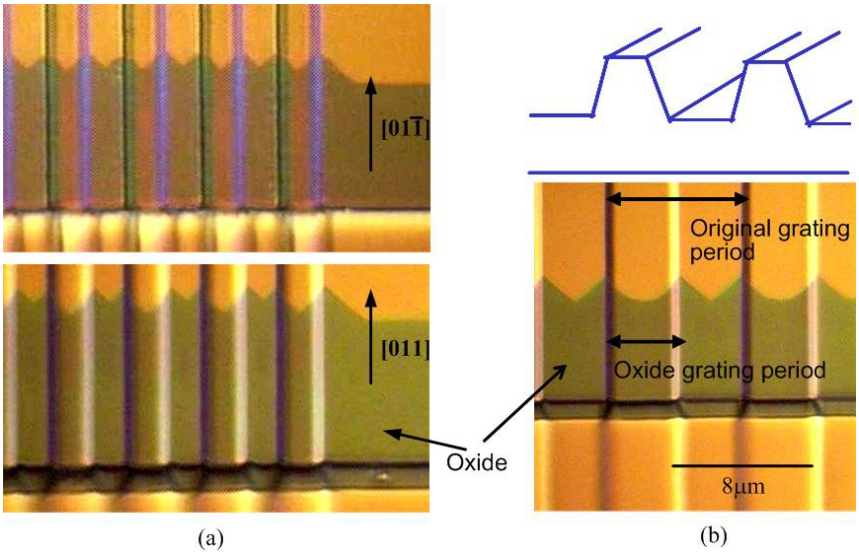

Fig. 3. (a) Oxidation front shows saw-tooth patterns both for $Al_xGa_{1-x}As$ along [01-1] and [011] trenches. (b) The comparison of the grating period before and after oxidation. The top schematic shows the grating geometry. The bottom is the bright field image of the oxide front. Trenches are [01-1] direction.

#1503 - $15.00 US Received July 29, 2002; Revised September 12, 2002

4. Device Applications

Two factors should be considered in designing a DFB structure using the AlOx grating. One is the grating order and the other is the coupling coefficient κ. An efficient DFB has $\kappa L \sim 1$ where L is the length of the device. To the leading order approximation, κ is proportional to $\int E^*(x)\Delta n^2(x)E(x)\mathrm{d}x$ where x is the direction of epitaxy and Δn is the index difference between the materials that make up the grating. An AlOx grating has a large $\Delta n \sim 1.9$ and κ can be easily controlled by the layer thickness between the grating and the active region.

To demonstrate the application, we fabricated a resonant-cavity-enhanced (RCE) photodetector. The device schematics and epi-structure are shown in Fig.4. The active region consisted of three $In_{0.2}Ga_{0.8}As$ 8nm/GaAs 10nm quantum wells. The first growth consisted of the bottom Si-doped $Al_{0.4}Ga_{0.6}As$ cladding, the active region, and 100nm each of undoped-GaAs and Zn-doped GaAs before we defined the grating. The resonant cavity had a length 75μm which was sandwiched by two DBR grating regions with 10 periods at the light-injection side and 66 pairs at the other side. The grating was defined along [01-1] direction and etched to 150nm depth. The overgrowth was comprised of two pairs of Zn-doped $Al_{0.97}Ga_{0.03}As$ / Zn-doped GaAs (24nm / 80nm) layers. The grating had a period of 2μm after oxidation. The order of the grating is 15 and has a coupling coefficient κ = 1.1 / cm at wavelength 930nm.

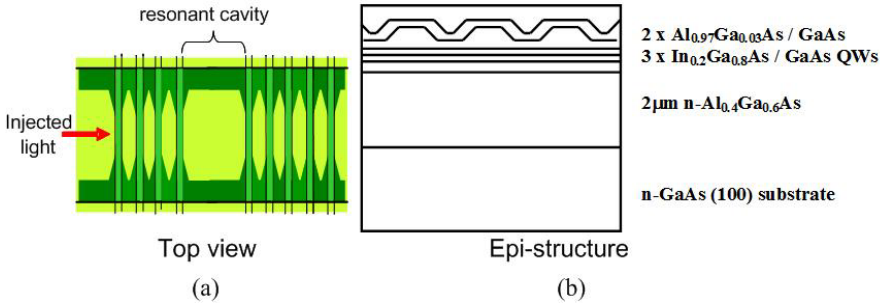

Fig. 4. Schematics of the RCE photodetector and the epi-structure.

The photocurrent responsivity as a function of input wavelength was measured using a semiconductor parameter analyzer (HP-4155) and a continuous-wave Ti-sapphire tunable laser. The result is shown in Fig.5 along with the simulation results with and without gratings. The experimental results qualitatively agreed with the simulation. Due to the grating period being too large compared to wavelength, limited by our optical lithography resolution, the coupling coefficient is very small. The efficiency can be increased by using a lower-order grating or reducing the distance between the AlOx layer and the active region. Further improvement of the performance will be investigated using higher-resolution lithography and reduction of the thickness between the active region and the AlOx grating.

#1503 - $15.00 US Received July 29, 2002; Revised September 12, 2002

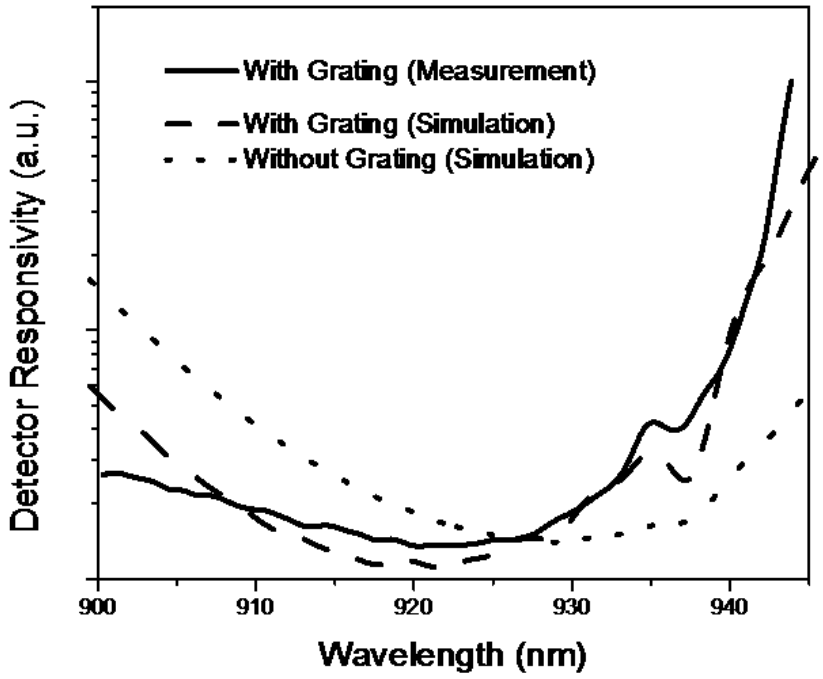

Fig. 5. Photocurrent responsivity spectrum versus injection light wavelength.

5. Conclusions

We proposed a novel buried AlOx/semiconductor horizontal cavity grating structure. Defect free high Al content $Al_xGa_{1-x}As$ grown on nonplanar substrates with $0.9 < x < 1$ was achieved using low-pressure MOCVD. After oxidation, we obtained a saw-tooth pattern oxide front with a period half of the original lithography defined pitch. An RCE photodetector structure was designed and fabricated using this AlOx grating as its DBR mirrors. This structure can find applications for making microcavity single-wavelength lasers and optoelectronic devices. Modeling of the growth profile and the oxidation pattern will be published later.

Acknowledgements

We would like to thank Ron Wilson and Kathy Buchheit for their assistance, and the staff of Microlab at University of California Berkeley, in particular Bob Hamilton and Robert Prohaska.

#1503 - $15.00 US Received July 29, 2002; Revised September 12, 2002